

## Response to Reviewer's Comments

**Manuscript Number:** acp-2018-800

**Authors:** Junfeng Wang, Dantong Liu, Xinlei Ge, Yangzhou Wu, Fuzhen Shen, Mindong Chen, Jian Zhao, Conghui Xie, Qingqing Wang, Weiqi Xu, Jie Zhang, Jianlin Hu, James Allan, Rutambhara Joshi, Pingqing Fu, Hugh Coe and Yele Sun

### Response to Reviewer #1

This manuscript belongs to the results of APHH 2016 winter campaign, it reports measurement results on the chemical properties of black carbon and the coating materials on the black carbon cores. It used a specific Aerodyne soot-particle aerosol mass spectrometry, which allows to analyze exclusively black-carbon containing particles. This technique avoids interferences from other non-BC containing particles, therefore can elucidate more accurately and directly the properties and evolution of BC in ambient air. Such type of measurement was for the first time conducted in wintertime Beijing, the data and results are thus very valuable. I agree its publication in ACP after some minor revisions suggested below:

**Authors' reply:** We thank the reviewer for his very positive feedback, and our point-to-point replies to the reviewer's comments are listed below.

(1) Is there any review paper to introduce this APHH campaign, and how does this paper contribute to the overall goal of this campaign? It should be mentioned.

**Authors' reply:** Yes, by the time of submission, the overview paper is not yet posted. It is now mentioned in the manuscript: Shi, et al.: Introduction to Special Issue – In-depth study of air pollution sources and processes within Beijing and its surrounding region (APHH-Beijing), Atmos. Chem. Phys. Discuss., <https://doi.org/10.5194/acp-2018-922>, 2018.

(2) The details of PMF analysis results were not mentioned, a diagnostic plot can be provided, at least in the attachment, to justify the choice of PMF solution.

**Authors' reply:** As requested by the reviewer, we have added a diagnostic plot of the PMF results as Fig. S2 in the supplement to justify the PMF results.

(3) Did the authors observe fullerene-related carbon cluster ions in the mass spectra of Beijing BC aerosols?

**Authors' reply:** Yes, we have observed fullerene-related carbon clusters during this campaign. In fact, we will publish the observation results regarding fullerenes from Beijing and also other sites in another paper, therefore we did not include them here

(4) Some modifications on the figures are necessary. For example, Font sizes in Fig 4 appear to be small; mass spectra in Fig.7 are less clear.

**Authors' reply:** As suggested, we have modified the figures (especially Figs. 4 and 7) to have a better quality.

(5) In Fig.6, the RBC ranges for clean and pollution periods are different, it is better to compare the variations on the same scale?

**Authors' reply:** In Figs.6c and 6d, the RBC ranges are set on the same scale.

(6) One general suggestion is that this dataset is unique as it measures only BC-particles in a highly polluted environment, the reviewer feels the discussion needs more comparisons with results in other locations or environments. As mentioned by the authors, such measurements were conducted in other sites in US, and Europe, even it is very scarce in China. This can help to show what is special or different or important of the findings observed in Beijing, and what are the implications of such findings to the atmospheric chemistry.

**Authors' reply:** Thanks for the suggestion. We in fact have included some comparisons with previous results including in Los Angeles, London, etc. during our discussion. Per the request, we have made some necessary minor changes in revising the manuscript. Please see the modified version for details.

### **Response to Reviewer #2**

BC also called as soot is an important aerosol from incomplete combustion of fossil fuels and biomass burning. Understanding the soot mixing state in polluted air of Beijing, it is quite important issue to evaluate their potential optical, hygroscopic, and human health. The authors used one SP-AMS to determine mixing state of soot particles collected in Beijing during the wintertime. They found coating/BC ratio was at 5.0, much smaller than highly aged soot in other places. Also, they studied coating chemical species and their possible formation mechanism. The scope of this study is suitable for ACP. However, the paper need to one substantial revision before it can be published. I list several concerns about the conclusions.

**Authors' reply:** We thank the reviewer for his valuable comments, and our point-to-point replies to the reviewer's comments are listed below.

(1) L28-29 deleted very (2) L30 only

**Authors' reply:** Done

(3) L33-34 how do the result indicate dominant contributions from primary emissions? You can say that these particles might source from local emissions instead of long-range transport particles. Am I right?

**Authors' reply:** We agree that this may not be appropriate, and we deleted this sentence.

(4) L35- 36, 38-40, seemly for me, the conclusion is contrast. One you mentioned primary emission. Other one you want to mention the secondary species.

**Authors' reply:** We agree with that the description is not very specific. In line with comment (3), we have modified the description. "Positive matrix factorization shows presence of significant primary fossil fuel and biomass burning organics."

(5) L41 at-during

**Authors' reply: done**

(6) L44-45, I don't think the conclusion is from your solid result. Most you speculate these results. (7) L44-47 the conclusion cover all the possible. I would ask the author revise it carefully. What is your conclusions during the sampling period. If these solid conclusions are not from this study, you need to remove it. Seemly, I like to see what you find on BC particles not for haze formation.

**Authors' reply:** The conclusions are based on our results, but are indeed only for BC-particles and two specific cases during the sampling period. We agree that over-interpretation should be avoided. Therefore, we have carefully revised this sentence. "However, for individual pollution events, sometimes primary species could also play a dominant role, as revealed by the compositions of BC-particles in two polluted episodes during the sampling period."

(8) L56 Morphology of BC might be altered greatly. These citations don't supply any morphology of BC particles. You need find others from electron microscopies.

**Authors' reply:** We have cited a couple of electron microscopic studies, including: Wang, Y., Liu, F., He, C., Bi, L., Cheng, T., Wang, Z., Zhang, H., Zhang, X., Shi, Z., and Li, W.: Fractal Dimensions and Mixing Structures of Soot Particles during Atmospheric Processing, *Environmental Science & Technology Letters*, 4, 487-493, 10.1021/acs.estlett.7b00418, 2017.

Li, W., Sun, J., Xu, L., Shi, Z., Riemer, N., Sun, Y., Fu, P., Zhang, J., Lin, Y., Wang, X., Shao, L., Chen, J., Zhang, X., Wang, Z., and Wang, W.: A conceptual framework for mixing structures in individual aerosol particles, *J. Geophys. Res. - Atmos.*, 121, 13,784-713,798, 10.1002/2016JD025252, 2016.

(9) L77, I don't agree with the claim. For example, Wu et al., 2017. Size distribution and source of black carbon aerosol in urban Beijing during winter haze episodes. *Atmos. Chem. Phys.* 17 (12), 7965-7975. The study seemly, give the online BC-containing particles in Beijing.

**Authors' reply:** Sorry, our claim is not clear, we meant to say that no chemical characterization of BC-containing particles only. It is now changed. And in fact, the work mentioned here was already cited as a previous work on BC-particles in Beijing.

(10) L161 Discussion, deleted s

**Authors' reply: done**

(11) L260-261, L284-285, L331-332 L347-348, all the parts discussed the aqueous reactions for nitrate and SOA formation during the nighttime. I take a look at the data from the study. It is too simply to get such conclusion. I might ask the authors cite more related references here. For example, Wu et al., 2018. *Environmental Science & Technology Letters* 5 (3), 160-166;Sun et al., 2018. *Journal of Geophysical Research: Atmospheres* 123 (2), 1234-1243.Kuang et al., 2016. *Geophysical Research Letters* 43 (16), 8744-8750.

**Authors' reply:** Thanks for the references provided. The aqueous-phase production of secondary species was a possible pathway in a qualitative manner. The references provided, which are also conducted in NCP, in fact strongly support our postulated aqueous-phase pathway therefore are very useful. They have now been cited along with our discussion in the main text. “Similarly, nitrate and sulfate formations driven by high RH in North China Plain have been proved previously (Kuang et al., 2016; Sun et al., 2018; Wu et al., 2018).”

(12) L278-279 I don't understand the sentence. Why was the large decrease of organics coating concentration?

**Authors' reply:** Since  $R_{BC}$  is the ratio of concentrations of total coating material to BC cores. There was a drop of  $R_{BC}$  at 4:00pm, however, since nitrate/BC, sulfate/BC and chloride/BC did not decrease around 4pm (there was even an increase of nitrate/BC), the decrease of  $R_{BC}$  must be caused by the decrease of organic/BC. And Fig.4f further shows that it is in fact the portions of BBOA and FFOA decreased since the OOA1/BC and OOA2/BC in fact increased. We have revised the sentence in the text. “In fact, the 4:00pm  $R_{BC}$  drop was mainly caused by the large decrease of Org/BC (as  $SO_4^{2-}/BC$ ,  $NO_3^-/BC$  and  $Cl^-/BC$  did not decrease at 4:00pm, Fig. 5d) - mainly the portions of fossil fuel and biomass burning OA (Fig. 4f). ”

(13) L292 at-during

**Authors' reply:** done

(14) L307 This can be expected for urban aerosols. I don't understand it. Why?

**Authors' reply:** We have expanded this sentence. “As BC-containing particle in urban Beijing were likely influenced by multiple local/regional primary sources, relative amount of secondarily formed coating species would be less than those of highly aged BC, therefore a lower  $R_{BC}$  is expected.”

(15) L328 of-at (16) L269 miss comma after ws (17) L317 at two polluted episodes

**Authors' reply:** done

(16) For section 3.5.2 Seemly, the authors found different coating species on soot particles. FE, the author found large SOA; SE the author proposed large POA instead of SOA. Do the authors answer how POA associated with BC? If these particles were emitted from sources, these mixing should occur in all the time, not just SE. Were there different sources in SE and FE? Seemly, the author didn't supply any wind and backtrajectories here. I would ask the authors carefully check the data. Make sure the differences in FE and SE are large. Here the authors only compared the organics. What about the sulfate and nitrate are in the coating of BC there. I am certainly struggling on the part.

**Authors' reply:** As requested, we have added the back trajectories, wind rose plots, as well as the vertical distributions of wind speeds/directions during these two episodes. It shows clearly that these episodes are very different, and therefore they would have

different sources. Yes, it is likely that a portion of the POA associated with BC might come from the sources (they mixed together with BC from the source), and such a portion might be present all the time. Nevertheless, what we try to demonstrate here is that: during FE, significant production of secondary species (likely from aqueous-phase reactions) of sulfate, nitrate and OOA1 led to the significant increase of BC-particles, while during SE, it was mainly the POA led to the extremely high loading of BC-particles. This can be seen clearly from the composition pie charts (Figs. 7a and 7b). Also, please note the major inorganic components including sulfate, nitrate, chloride and ammonium were also shown. Increases of inorganic species were also observed during FE not only organics, while during SE, inorganic species were significantly lower than those of the average case. We have modified the writing to make our arguments clear and straightforward.

**Characterization of black carbon-containing fine particles  
in Beijing during wintertime**

Junfeng Wang<sup>1</sup>, Dantong Liu<sup>2</sup>, Xinlei Ge<sup>1\*</sup>, Yangzhou Wu<sup>1</sup>, Fuzhen Shen<sup>1</sup>, Mindong Chen<sup>1</sup>, Jian Zhao<sup>3,4</sup>, Conghui Xie<sup>3,4</sup>, Qingqing Wang<sup>3</sup>, Weiqi Xu<sup>3,4</sup>, Jie Zhang<sup>5</sup>, Jianlin Hu<sup>1</sup>, James Allan<sup>2,6</sup>, Rutambhara Joshi<sup>2</sup>, Pingqing Fu<sup>3</sup>, Hugh Coe<sup>2</sup> and Yele Sun<sup>3,4</sup>

<sup>1</sup>Jiangsu Key Laboratory of Atmospheric Environment Monitoring and Pollution Control, School of Environmental Science and Engineering, Nanjing University of Information Science and Technology, Nanjing 210044, China

<sup>2</sup>School of Earth and Environmental Sciences, University of Manchester, M13 9PL, Manchester, UK

<sup>3</sup>State Key Laboratory of Atmospheric Boundary Layer Physics and Atmospheric Chemistry, Institute of Atmospheric Physics, Chinese Academy of Sciences, Beijing 100029, China

<sup>4</sup>University of Chinese Academy of Sciences, Beijing 100049, China

<sup>5</sup>Atmospheric Sciences Research Center, University at Albany, State University of New York, NY, 12203, USA

<sup>6</sup>National Centre for Atmospheric Science, University of Manchester, M13 9PL, Manchester, UK

\*Corresponding author, Email: caxinra@163.com

Phone: +86-25-58731394

*For Atmospheric Chemistry & Physics*

## Abstract

Refractory black carbon (BC) is a product from incomplete combustion of fossil fuel, biomass and biofuel, etc. By mixing with other species, BC can play significant roles in climate change, visibility impairment and human health. Such BC-containing particles in ~~very~~-densely-populated megacities, like Beijing, may have specific sources and properties, that are ~~very~~-important to ~~the~~ haze formation and air quality. In this work, we characterized exclusively the BC-containing particles ~~only~~ in urban Beijing, by using a laser-only Aerodyne soot particle aerosol mass spectrometer (SP-AMS), as a part of the Air Pollution and Human Health (APHH) 2016 winter campaign. The average mass ratio of coating-to-BC ( $R_{BC}$ ) was found to be  $\sim 5.0$ , ~~much smaller than those of highly aged BC, indicating dominant contributions from primary emissions.~~ Positive matrix factorization ~~indeed~~ shows ~~the dominance~~presence of significant primary fossil fuel and biomass burning organics- (64% of total organics). Yet secondary species, including ~~both~~ sulfate, nitrate and oxygenated organic aerosol (OA) species, could have significant impacts on the properties of BC-containing particles, especially for ones with larger BC core sizes and thicker coatings. Analyses of ~~the~~ sources and diurnal cycles of organic coating reveal significant afternoon photochemical production of secondary OA (SOA), as well as ~~the~~-nighttime aqueous production of a portion of highly oxygenated OA. Besides SOA, photochemical production of nitrate, not sulfate, ~~was very~~appeared to be important. Further investigations on BC-containing particles ~~at~~during different periods show that, on average, more polluted periods would have more contributions from secondary species, and more thickly coated BC tended to associate with more secondary species, indicating the important role of chemical aging to the ~~air~~-pollution of BC-containing particles in urban Beijing during wintertime. However, for individual pollution events, ~~aqueous phase production of sulfate, nitrate and SOA might aggravate the pollution obviously under high relative humidity conditions, while sometimes local primary emissions (species (fossil fuel, coal and biomass burning emissions) could lead to serious and extremely~~also play a dominant role, as revealed by the compositions of BC-particles in two polluted ~~event too~~-episodes during the sampling period.

## 1. Introduction

Black carbon (BC) is generated from incomplete combustion of carbon-based fuels (Ramanathan and Carmichael, 2008), and can exert significant impacts on global and regional climate, planetary boundary layer height (PBLH), air quality and human health, etc. (Lee et al., 2017; Bond et al., 2013; Ding et al., 2016). BC can strongly absorb solar radiation and warm up the atmosphere directly. By internally or externally mix with non-BC materials (coatings, including co-emitted primary organics/inorganics and secondary materials that associate with BC) (Chen et al., 2016a; Lee et al., 2017; Wang et al., 2017a), the properties and morphologies of BC might be altered greatly (Liu et al., 2013; Liu et al., 2017; Liu et al., 2015; Cappa et al., 2012; Peng et al., 2016; Wang et al., 2017c; Li et al., 2016). Thick coating can increase the mass absorption cross section of BC, thus enhance the light absorption of BC core via “lensing effect” (Jacobson, 2011; Liu et al., 2015; Pokhrel et al., 2017). However, coating thickness of BC-containing particles significantly depends on ~~their~~ sources/chemical ~~composition~~compositions and aging processes, thus there are great uncertainties on light absorption enhancement ( $E_{\text{abs}}$ ) of BC as well as its global radiative forcing (Cappa et al., 2012; Liu et al., 2017; Cui et al., 2016; Liu et al., 2015). For instance, the mass ratio of coatings to BC core ( $R_{\text{BC}}$ , an analog of coating thickness) from biomass burning is usually greater than 3 (Liu et al., 2017) and can be larger than 10 in remote sites (Wang et al., 2017a). Normally, when  $R_{\text{BC}}$  is less than 1.5, it is probably from traffic sources, whereas secondary organic aerosol (SOA) dominated BC-containing particles is usually with a  $R_{\text{BC}}$  greater than 4 (Lee et al., 2017). Moreover, the coating species can modify the hygroscopicity of BC-containing particles (Liu et al., 2013) when associated with hydrophilic materials, and some of them can ~~serve as~~activated into cloud condensation nuclei (CCN), therefore alter the albedo and precipitation of clouds indirectly (Dusek et al., 2010; Dusek et al., 2006).

In the past decades, a number of field studies on BC have been conducted in the winter of Beijing, and mainly focused on BC mass loadings, mixing states, optical properties, human health impacts and sources (coal combustion, biomass burning and vehicles, etc.) (Wu et al., 2017; Cheng et al., 2017; Ji et al., 2017; Wang et al., 2017b; Wu et al., 2016; Chen et al., 2016b; Meng et al., 2016; Wang et al., 2016b; Liu et al., 2016; Yang et al., 2014; Schleicher et al., 2013a; Schleicher et al., 2013b; Song et al., 2013; Zhang et al., 2017). There were real-time studies on BC, and on the chemical characteristics of total fine particles (including particles with and without BC) in Beijing. However, to the best of our knowledge, no study was conducted in real-time to characterize the chemical compositions exclusively



~~only of~~ BC-containing particles in Beijing despite the important effects of coating materials on BC properties aforementioned. Currently, a few studies have explored BC-containing particles in other locations, e.g., Toronto (Willis et al., 2016; Lee et al., 2015), California (Lee et al., 2017; Massoli et al., 2015; Cappa et al., 2012), London (Liu et al., 2015) and Tibet (Wang et al., 2017a) by using the Aerodyne soot-particle Aerosol Mass Spectrometer (SP-AMS) (Onasch et al., 2012; Lee et al., 2015; Wang et al., 2016a; Ge et al., 2017b). The SP-AMS physically combines the 1064 nm laser vaporizer of single particle soot photometer (SP2) into a high-resolution aerosol mass spectrometer (HR-AMS) ~~(Onasch et al., 2012; Canagaratna et al., 2007).~~. After removal of the AMS tungsten vaporizer and by operating the instrument with ~~the~~ laser vaporizer only, refractory BC as well as its associated coating can be evaporated since the 1064 nm laser can selectively heat the BC (Massoli et al., 2015). In other words, ~~the~~ laser-only SP-AMS can exclusively measure BC cores and the species coated on BC cores. This unique technique allows us to explore in details the characteristics of BC-coating species with no perturbations from other co-existing non-BC containing particles in ambient air.

Beijing, as the most reprehensive megacity with a large population in developing countries, the BC-containing particles may have specific source profiles and physiochemical properties, therefore elucidation of its characteristics is important to understand the haze formation and improve air quality in such regions. ~~In this work,~~ In this work, as a part of the UK-China Air Pollution and Human Health (APHH) study (Shi et al., 2018), we report for the first time the real-time measurement results on the chemical composition, mass loading, size distribution, and sources/processes of ~~the~~ BC-containing particles during wintertime of 2016 in urban Beijing ~~by using the laser only SP-AMS.~~ Results regarding ~~mixing states physical properties~~ and optical properties are presented in ~~other publications~~ in Liu et al. (2018) and Xie et al. (2018) of this special issue-, respectively.

## 2. Experiments

### 2.1 Sampling site and instrumentation

As a part of the ~~UK CHINA Air Pollution & Human Health (APHH)~~ winter campaign, we conducted measurements at the Tower Division of Institute of Atmospheric Physics (IAP), Chinese Academy of Science (39°58'N, 116°22'E) in Beijing (Figure S1 in the supplement), from 15 November to 13 December of 2016. The site was surrounded by residential infrastructures and a freeway in the east (360m).

113 The SP-AMS was deployed on the rooftop of Herong Building (~8m above the ground), with a  
114 PM<sub>2.5</sub> cyclone (Model URG-2000-30EN) and a diffusion dryer in front of the inlet. The single particle  
115 soot photometer (SP2, Droplet Measurement Technology, Inc., Boulder, CO, USA) was operated  
116 simultaneously ~~nearby~~ inside another container nearby (~20 m away) on the ground. The SP2  
117 incandescence signal was calibrated for BC mass by using Aquadag® black carbon standard (Aqueous  
118 Deflocculated Acheson Graphite, Acheson Inc., USA) (Laborde et al., 2012). For the SP-AMS, since  
119 the filament that ejects electrons can still heat the tungsten vaporizer up to ~200 °C (Willis et al., 2014)  
120 even it is turned off, the tungsten vaporizer was thus physically removed to make sure only BC and its  
121 associates were vaporized by the laser, and to eliminate influences from species uncoated on ~~the~~ BC  
122 cores.

123 The tuning and calibration procedures of ~~the~~ SP-AMS followed the procedures described  
124 previously (Lee et al., 2015; Willis et al., 2016; Massoli et al., 2015; Wang et al., 2017a). During the  
125 campaign, the SP-AMS was run with a 10-minutes cycle: one W mode with high chemical resolution  
126 (2.5 min) and two mass sensitive V modes including one with particle time of flight (PToF) mode (2.5  
127 min) and another one (5 min) with the measured a large mass-to-charge ( $m/z$ ) range (up to 2000 ~~to~~  
128 investigate fullerene-like carbon clusters) (Wang et al., 2016a). The filtered air measurement was  
129 performed for a day to determine the detection limits (DLs) of various aerosol species and to adjust  
130 the fragmentation table. The ionization efficiency (IE) and relative ionization efficiency (RIE) of  
131 sulfate and nitrate were calibrated by using pure ammonium nitrate and ammonium sulfate according  
132 to Jayne et al. (2000), respectively. RIE of BC was calibrated by using Regal Black (RB, REGAL 400R  
133 pigment black, Cabot Corp.) (Onasch et al., 2012), and the average ratio of C<sub>1</sub><sup>+</sup> to C<sub>3</sub><sup>+</sup> was determined  
134 to be 0.53 to minimize the influence of C<sub>1</sub><sup>+</sup> from non-refractory organics. However, it should be aware  
135 that laser-only SP-AMS cannot vaporize ammonium nitrate/sulfate if they do not coat on BC, thus the  
136 IE and RIE calibrations were done before removal of the tungsten vaporizer and the values were  
137 assumed to be unchanged after the tungsten heater's removal (Willis et al., 2016). Note the RIE of BC  
138 was calibrated before the campaign and was repeated in the middle and end of the campaign. RIEs of  
139 nitrate, ammonium, sulfate and BC were determined to be 1.1, 3.82, 0.82, and 0.17, respectively. The  
140 default value of 1.4 was used as RIE of organics (Canagaratna et al., 2007). Polystyrene latex (PSL)  
141 spheres (100-700 nm) (Duke Scientific Corp., Palo Alto, CA) were used to calibrate the size before  
142 the campaign (Canagaratna et al., 2007) .

## 2.3 Data Analysis

Standard AMS data analysis software (Squirrel and Pika) based on Igor Pro 6.37 (Wavemetrics, Lake Oswego, OR, USA) were used to obtain the concentrations, mass spectra and size distributions of BC and its coating species. All data were calculated based on high-resolution fitting results. Due to different vaporization schemes between the SP-AMS and HR-AMS, mass spectra from these two instruments even for the same population of particles are not entirely the same. Laser-only SP-AMS can result in overall less fragmentation, therefore the mass profile may contain more large  $m/z$  fragments and less small  $m/z$  fragments compared with that from HR-AMS (Massoli et al., 2015). Therefore, here the elemental ratios of organics, i.e., oxygen-to-carbon, hydrogen-to-carbon and nitrogen-to-carbon ratios (O/C, H/C and N/C) were determined by the Aiken approach first (Aiken et al., 2008), and then O/C and H/C were corrected by using factors of 0.83 and 1.16, respectively (Canagaratna et al., 2015).

Source apportionment for organics coated on BC was conducted by using Positive matrix factorization (PMF) (Paatero and Tapper, 1994) Evaluation Tool written in Igor (Ulbrich et al., 2009). In this study, high-resolution mass spectra (HR-MS) of organic (including BC) and inorganic species were combined together to perform the PMF analyses (Sun et al., 2012; Wang et al., 2017a; Wang et al., 2018). It should be noticed that, only fragment ions from polycyclic aromatic hydrocarbons (PAHs) were included for  $m/z$  range of ~150 to ~250 in the PMF analysis because of the limited mass resolution of SP-AMS. All PMF solutions were evaluated following the standard instruction (Zhang et al., 2011). Finally, four types of organic aerosol (OA) associated with BC were determined eventually, including a fossil fuel combustion OA (FFOA), a biomass burning OA (BBOA) and two oxygenated OA (OOA1 and OOA2) (a diagnostic plot was provided in Fig. S2).

Supporting data such as meteorological parameters including relative humidity (RH), wind speed (WS), wind direction (WD) and temperature (T), as well as concentrations of gaseous species such as O<sub>3</sub>, SO<sub>2</sub>, NO, NO<sub>2</sub>, NO<sub>x</sub>, NO<sub>y</sub>, NO<sub>z</sub>, and CO were measured in parallel simultaneously. All data reported here were at local time (Beijing Time, UTC+8).

## 3. Results and ~~discussions~~discussion

### 3.1 Overview of BC-containing aerosol characteristics

Figs. 1 and 2 show the temporal variations of meteorology parameters, mass loadings of gaseous

173 pollutants (CO, NO<sub>x</sub>, SO<sub>2</sub> and O<sub>3</sub>), BC and its associated coating components (sulfate, nitrate,  
174 ammonium, chloride, total OA and ~~the~~ four PMF-resolved OA factors). The campaign-averaged  
175 composition of BC-containing particles and mass contributions of the four OA factors to total OA were  
176 also displayed in Fig. 2. Overall, wind directions and speeds had close associations with ~~the~~ overall  
177 mass loadings of BC-containing particles. The pollution periods (characterized by concentrations of  
178 BC-containing particles above 10 µg m<sup>-3</sup>) were accompanied by relatively low wind speeds (<4 m s<sup>-1</sup>)  
179 and in a relatively large part from southern air masses since Beijing is at the foot of the mountains  
180 which facilitate the accumulation of pollutants from southern North China Plain (NCP). The clean  
181 periods (characterized by the concentrations of BC-containing particles below 10 µg m<sup>-3</sup>) were mainly  
182 under the control of northwest strong winds (>4 m s<sup>-1</sup>) ~~from the northwest~~ (Fig. S3). During the  
183 campaign, the mass loadings of BC cores and BC-containing particles ranged from 0.11 ~26.54 µg m<sup>-3</sup>  
184 <sup>3</sup> and 0.71~174.40 µg m<sup>-3</sup>, with an average of 4.9 µg m<sup>-3</sup> and 29.4 µg m<sup>-3</sup>, respectively. We also  
185 compared BC concentrations determined by the SP-AMS with those from SP2, and they correlated  
186 quite well with each other (*r*<sup>2</sup> of 0.93; Fig. S3S4), indicating the quantification of BC by the SP-AMS  
187 is reliable.

188 The coating species occupied on average about 83.4% of the mass of BC-containing particles,  
189 indicating BC was generally thickly coated throughout the whole campaign, with an average mass  
190 ratio of coatings to BC (*R*<sub>BC</sub>) of ~5.0. Organic aerosol (OA) was the most abundant coating component,  
191 taking up to 59.4% of the total mass, followed by nitrate ~~(8.8%)~~, sulfate ~~(6.5%)~~, ammonium ~~(4.7%)~~  
192 and chloride ~~(8.8%, 6.5%, 4.7% and 4.0%, respectively)~~ ~~(%)~~. OA correlated quite well with BC (*r*<sup>2</sup> of  
193 0.97), suggesting that many OA species were co-emitted and mixed with BC, and indeed, primary OA  
194 (POA=FFOA+BBOA) was found to dominate the OA mass (66.3%=43.9%+22.4%). Chloride (Cl<sup>-</sup>)  
195 had a great correlation with BC (*r*<sup>2</sup> of 0.94), suggesting it was mainly associated with primary  
196 emissions, for example, gasoline, diesel and coal combustion during wintertime in urban Beijing.  
197 Sulfate and nitrate are typically secondarily formed, therefore their correlations with BC were  
198 relatively weak (*r*<sup>2</sup> of 0.64 for SO<sub>4</sub><sup>2-</sup> vs. BC, and 0.60 for NO<sub>3</sub><sup>-</sup> vs. BC). Their properties are discussed  
199 in ~~more~~ details in the following sections.

### 200 201 3.2 Chemically-resolved size distributions of BC-containing particles

202 Fig. 3a shows the campaign-averaged mass-based size distributions of major BC-coating species,

带格式的: 字体: 非倾斜

带格式的: 字体: 非倾斜

including organics (BC-Org), sulfate (BC-Sulfate), nitrate (BC-Nitrate), chloride (BC-Chl) and BC core itself. It should be noticed that the size distribution of BC was scaled from that of  $m/z$  24 ( $C_2^+$ ), as other major carbon cluster ions might be significantly affected by other ions, for example,  $C_1^+$  at  $m/z$  12 can be influenced by fragments from non-BC organics,  $C_3^+$  at  $m/z$  36 by  $HCl^+$ ,  $C_4^+$  at  $m/z$  48 by  $SO^+$ , and  $C_5^+$  at  $m/z$  60 by  $C_2H_4O_2^+$  etc. Similarly, the size distribution of BC-Chl was scaled from  $Cl^+$  signal at  $m/z$  35. As shown in Fig. 3a, on average, size distributions of BC-Sulfate, BC-Nitrate and BC-Org displayed a similar pattern with a major peak at  $\sim 550$  nm (vacuum aerodynamic diameter,  $D_{va}$ ), suggesting that they were relatively well internally mixed. However, the BC presented a remarkably different pattern with a much broader distribution and smaller peak sizes than its coating species, and in particular, relatively small particles tended to have thin coatings.

Figs. 3b-f further present image plots of size distributions of the major aerosol components as a function of  $R_{BC}$  (as a surrogate for coating thickness). Different from the average data shown in Fig. 3a, the coating species can be roughly classified into two modes separated by  $R_{BC}$  of  $\sim 4.5$ . Most sulfate and nitrate concentrated at  $R_{BC} > 4.5$  (Figs. 3b and 3c): Sulfate peaked in a narrow  $R_{BC}$  range of 5.5–6.5, while significant nitrate mass could distribute across a wider  $R_{BC}$  range (even to  $R_{BC}$  of  $\sim 8.0$ ). Only organics and chloride had a significant portion of mass distributed on relatively thinly coated BC-containing particles at  $R_{BC} < 4.5$  (Figs. 3e and 3f). Specifically, they both showed a sub-mode locating in the regime with  $R_{BC}$  of  $\sim 3.5$ –4.5 and  $D_{va}$  of  $\sim 200$ –700 nm. These sub-modes suggest that organics or chloride are partially from primary sources as freshly emitted BC are more likely thinly coated. This is consistent with that organics included species from fossil fuel and biomass burning combustion revealed by the PMF analysis. Similarly, coal burning might contribute to chloride during wintertime in Beijing (Sun et al., 2016). As for sulfate and nitrate, since they are predominantly secondary species, they would coat on BC cores due to chemical aging therefore mostly distributed at higher  $R_{BC}$ .

### 3.3 Sources of organic coating species

The high-resolution mass spectra (HRMS) of different factors of the organic coating resolved from PMF analyses, their relative contributions and diurnal cycles of temporal variations relative to BC are shown in Fig. 4. Fig. 4a illustrates the mass profile of the fossil fuel combustion OA with BC carbon clusters (FFOA + BC). This factor had a low O/C ratio of 0.16. In this work, this factor might include emissions from both traffic and coal combustion, as it contained a series of significant PAHs ion

带格式的: 字体: 非倾斜

带格式的: 字体: 非倾斜

233 fragments in the mass spectrum (PAHs fragments are negligible in other factors) indicative of coal  
234 burning (Sun et al., 2014; Sun et al., 2016), and presented a good correlation with  $C_4H_9^+$  ( $r^2$  of 0.72)  
235 ~~which is~~ a AMS tracer ion of vehicle emissions (Zhang et al., 2005). Temporal variations of FFOA  
236 also correlated well with  $C_9H_7^+$  ( $m/z$  115,  $r^2$  of 0.92) and  $Cl^-$  ( $r^2$  of 0.60), which have been proposed as  
237 possible coal combustion tracer species (Yan et al., 2018; Sun et al., 2014). The FFOA/BC (Fig. 4f)  
238 appeared to be higher during nighttime than that during daytime. Note the diurnal pattern of BC itself  
239 (Fig. 5c) was similar as that of FFOA/BC. The diurnal variations of BC might be influenced by both  
240 fossil fuel combustion activities and relatively low PBLH during nighttime. The fossil fuel combustion  
241 included coal burning and vehicle emissions (gasoline cars, and the heavy-duty diesel vehicles that are  
242 only allowed to enter the city during later night). The mass ratios of different factors to BC shall have  
243 less influences from PBLH, therefore high levels of FFOA/BC strongly indicate that co-emitted  
244 organic species with BC from fossil fuel combustion were enhanced during nighttime.

245 Figure 4b shows the mass spectrum of BBOA and related BC clusters. One feature of this factor  
246 is that it had relatively high fractional contributions of  $C_2H_4O_2^+$  (1.47% of total) and  $C_3H_5O_2^+$  (0.95%),  
247 which are often regarded as AMS marker ions from biomass burning emitted levoglucosan (Cubison  
248 et al., 2011; Mohr et al., 2009). Note the FFOA also contained appreciable  $C_2H_4O_2^+$  and  $C_3H_5O_2^+$   
249 signals, partially due to that coal burning (such as lignite) can emit some levoglucosan as well (Yan et  
250 al., 2018). Nevertheless, mass fractions of  $C_2H_4O_2^+$  and  $C_3H_5O_2^+$  in FFOA were less than those in  
251 BBOA, and they correlated much better with BBOA than those with FFOA (for examples,  $r^2$  of 0.90  
252 for BBOA vs.  $C_2H_4O_2^+$ , and 0.72 for FFOA vs.  $C_2H_4O_2^+$ ). The BBOA correlated very well with another  
253 biomass burning tracer -  $K^+$  ( $r^2$  of 0.90). In addition, BBOA had negligible PAHs ion fragments while  
254 the FFOA contained remarkably high PAHs signals. Such characteristics are generally in agreement  
255 with previous AMS findings in the same location during wintertime in Beijing (Sun et al., 2016). For  
256 these reasons, the second factor was identified as BBOA. The diurnal pattern of BBOA/BC reached  
257 minimum during afternoon and was overall high during nighttime, similar as FFOA/BC, indicating the  
258 nighttime enhancement of BB-related organics emissions in wintertime Beijing.

259 Besides the two POA factors, we also identified two secondary OA factors (OOA1 and OOA2),  
260 whose O/C ratios were 0.45 and 0.28, respectively. OOA1 was the most oxidized OA factor that had a  
261 higher  $CO_2^+/C_2H_3O^+$  ratio than that of OOA2. The correlation between OOA1 and sulfate was better  
262 than it with nitrate ( $r^2$  of 0.99 vs. 0.86). As a comparison, the less oxygenated OOA2 correlated better

263 with nitrate than it with sulfate ( $r^2$  of 0.59 vs. 0.34). These characteristics are consistent with previous  
264 AMS-PMF results (Zhang et al., 2011). Opposite to the diurnal cycles of FFOA and BBOA, the  
265 OOA2/BC ratio arose significantly from early morning and peaked in the afternoon (~3pm). The  
266 diurnal pattern of OOA1/BC presented a similar peak at ~3pm. This result demonstrates a clear  
267 evidence and important role of afternoon photochemical reactions to the formation of secondary  
268 organic species. However, the precursors leading to the formations of OOA1 and OOA2 remain to be  
269 elucidated. Interestingly, for OOA1/BC, in addition to the peak during afternoon, ~~the ratio it~~ increased  
270 during early evening and remained at high levels until early morning. This result indicates that  
271 nighttime aqueous-phase processing (high levels of RH during nighttime shown in Fig. 5a) can also  
272 contribute to OOA1 production. As such behavior was not observed for OOA2/BC, it agrees with  
273 previous field and laboratory findings that aqueous-phase reactions tend to produce more highly  
274 oxygenated species (Ervens et al., 2011; Ge et al., 2012; Herrmann et al., 2015; Xu et al., 2017).

275 Overall, the mass fractions of BC cores that were associated with fossil fuel combustion, biomass  
276 burning, less and more oxygenated secondary processes were 32.7%, 31.8%, 18.7% and 16.9%,  
277 respectively (Fig. 4e). The organic coating of BC was predominantly ~~coated by~~ primary species.

### 279 3.4. Diurnal patterns of BC and coating species

280 Fig. 5 presents the diurnal cycles of meteorological parameters (T, RH, WS and WD), BC  
281 concentrations and  $R_{BC}$ , mass ratios of major species to BC, gaseous species (CO, SO<sub>2</sub> and NO<sub>x</sub>), O/C  
282 and OS<sub>c</sub> (oxidation state, defined as  $2 \times O/C-H/C$ ) (Kroll et al., 2011). Note BC did not present a peak  
283 at 8:00 am, yet  $R_{BC}$ , Org/BC, SO<sub>4</sub><sup>2-</sup>/BC, NO<sub>3</sub><sup>-</sup>/BC and Cl<sup>-</sup>/BC were all low at ~8:00 am. This was likely  
284 attributed to increase of the mass fractions of fresh and barely coated BC-containing particles (rather  
285 than the increase of absolute concentrations of fresh BC-containing particles) emitted during morning  
286 rush hours from traffic emissions, etc. This was consistent with the decreases of O/C and OS<sub>c</sub> and  
287 increases of CO and NO<sub>2</sub> at 8:00 am of the day. On the contrary, the  $R_{BC}$  drop at ~4:00 pm was unlikely  
288 due to influences of afternoon rush hours, as there were no increases of CO, NO<sub>2</sub>, and both O/C and  
289 OS<sub>c</sub> were at high levels. In fact, the 4:00pm  $R_{BC}$  drop was mainly caused by the large decrease of  
290 ~~organics coating concentration~~ Org/BC (as SO<sub>4</sub><sup>2-</sup>/BC, NO<sub>3</sub><sup>-</sup>/BC and Cl<sup>-</sup>/BC did not decrease at 4:00pm,  
291 Fig. 5d) - mainly the portions of fossil fuel and biomass burning OA (Fig. 4f).

292 The diurnal variation of NO<sub>3</sub><sup>-</sup>/BC peaked at ~3-4 pm, consistent with the variation of T, and similar

带格式的: 字体: 非倾斜

as those in the previous reports during wintertime in Beijing (Ge et al., 2017a; Sun et al., 2016), reflecting the dominated contribution of photochemical formation of nitrate.  $\text{SO}_4^{2-}/\text{BC}$  showed a relatively small afternoon increase, indicating partial sulfate was produced from photochemical activities; it also presented a nighttime enhancement, similar as  $\text{OOA1}/\text{BC}$ , suggesting the sulfate formation in aqueous-phase, consistent with the nighttime increase of RH and decrease of temperature (Fig. 5a). Due to increases of  $\text{FFOA}/\text{BC}$ ,  $\text{BBOA}/\text{BC}$  and  $\text{OOA1}/\text{BC}$  (the portion likely from aqueous-phase production),  $\text{Org}/\text{BC}$  remained at high levels during nighttime. All these increases added together, leading to the high  $R_{\text{BC}}$  during nighttime. In addition,  $\text{Cl}/\text{BC}$  varied generally similar to those of  $\text{FFOA}/\text{BC}$  and  $\text{BBOA}/\text{BC}$ , again indicating its strong association with primary emissions.

### 3.5 Characteristics of coating species during different periods

#### 3.5.1 Coating compositions ~~at~~during clean and pollution periods

Fig. 6 shows the variations of BC-coating compositions as a function of ~~coating thickness~~ $R_{\text{BC}}$  during clean (CP) and pollution periods (PP) (~~separated~~divided by the concentration of  $10 \mu\text{g}/\text{m}^3$ ), respectively. Contrasting difference of the coating composition during these two cases was observed: primary OA (especially FFOA) appeared to be the most abundant component during CP while mass contributions of secondary organic and inorganic species were remarkably high during PP (Figs. 6a and b), and the average  $R_{\text{BC}}$  during PP ( $\sim 5.1$ ) was also higher than that during CP ( $\sim 4.5$ ) (Fig. 6f). These results again reinforce the importance of secondarily formed species to the heavy haze pollution in urban Beijing (Huang et al., 2014). Furthermore, the BC coating composition as well as  $\text{OS}_c$  during CP were both relatively stable against  $R_{\text{BC}}$  (Fig. 6c). On the contrary, during PP, with the increase of  $R_{\text{BC}}$ , the mass fractions of secondary species (OOA1, nitrate and sulfate) increased clearly, especially at  $R_{\text{BC}} > 5$ ; consistently,  $\text{OS}_c$  of organic coating increased from  $\sim 0.85$  to  $> 0.70$ . Such behavior again highlights the contribution of chemical aging process to the heavy haze pollution.

Relative to other observations (Wang et al., 2017a; Massoli et al., 2015; Cappa et al., 2012), the levels of  $R_{\text{BC}}$  during both CP and PP are much smaller than those for highly aged BC, which might have  $R_{\text{BC}} > 10$ . ~~This can~~As BC-containing particle in urban Beijing were influenced by multiple local/regional primary sources, relative amount of secondarily formed coating species would be less than those of highly aged BC, therefore this lower  $R_{\text{BC}}$  is expected for urban aerosols. On the other hand, the  $R_{\text{BC}}$  levels ~~here are also~~ generally higher than those found for the BC-containing particles in

带格式的: 下标



Los Angeles where the average  $R_{BC}$  was typically smaller than 4 due to ~~predominant~~direct and prominent influence of vehicle emissions (Lee et al., 2017). Regarding the variations of coating composition vs.  $R_{BC}$ , the behavior during PP is in fact consistent with a few previous field measurement results in American or European urban locations (Massoli et al., 2015; Liu et al., 2017; Lee et al., 2017; Cappa et al., 2012; Collier et al., 2018), indicating a general behavior for BC-containing particles in urban area that more aged BC tends to have thicker coating. Yet this property can be altered if significant POA emissions exist, such as the case during CP in this work, and a case with heavy BBOA influences observed in Tibet Plateau (Wang et al., 2017a).

### 3.5.2 Coating compositions ~~at~~during two different episodes

Although we demonstrated in Section 3.5.1, the heavy pollution of BC-containing particles was on average associated with more secondary species, the underlying governing factors of individual pollution events might vary from each other. Here we investigated the characteristics of BC-containing particles in two most polluted episodes occurring during the campaign. The first episode (FE) was accompanied with relatively high RH (from 6:00 pm of 3 Dec. to 8:00 am of 4 Dec., 2016), while the second episode (SE) was dominated by primary emissions (from 0:00 am to 6:00 am of 11 Dec., 2016). The average mass loadings of BC cores and BC-containing particles were  $18.1 \mu\text{g m}^{-3}$  and  $123.1 \mu\text{g m}^{-3}$  during FE,  $14.4 \mu\text{g m}^{-3}$  and  $80.0 \mu\text{g m}^{-3}$  during SE, respectively - both were much higher than the campaign-averaged BC of  $4.9 \mu\text{g m}^{-3}$  and BC-containing particles of  $29.4 \mu\text{g m}^{-3}$ . Back trajectories, wind rose plots and distributions of the wind speeds/directions of these two episodes were provide in Fig. S5, showing that these two episodes had remarkably different air mass origins and sources.

For FE, the average T and RH were  $\sim 4.2^\circ\text{C}$  and  $\sim 78\%$ , respectively. The average T was close to the campaign-average value of  $4.8^\circ\text{C}$ , but the air was more humid than the campaign-average RH of  $\sim 50\%$ . Correspondingly, we observed ~~clear increases~~remarkable elevations of the mass contributions of sulfate from 6.5% to 10.3%, nitrate from 8.8% to 10.2%, OOA1 from 7.5% to 11.5% (Figs. 7a and 7c). Such enhancements were very likely linked with the aqueous-phase processing as this episode occurred during nighttime and was characterized with high RH conditions. During FE, nitrate and sulfate also correlated very well ( $r^2$  of 0.94; Fig. ~~S4~~S6), therefore formation of nitrate would also relate with aqueous-phase processing in this episode. Consistently, nitrate and sulfate formations driven by high RH in North China Plain have been proved previously (Kuang et al., 2016; Sun et al., 2018; Wu

et al., 2018). As a comparison, the mass fraction of photochemical-relevant OOA2 decreased significantly from campaign-average 13.3% to 9.8%. In addition, mass fraction of Cl<sup>-</sup> also increased from campaign-average 4.0% to 5.3%; meanwhile, we found that relative to the campaign-average values, the KCl<sup>+</sup>/BC ratio decreased 14%, the K<sub>3</sub>SO<sub>4</sub><sup>+</sup>/BC ratio increased 28%, possibly indicating that the heterogeneous replacement reactions of coal-burning related Cl<sup>-</sup> by SO<sub>4</sub><sup>2-</sup> during FE (Fig. S4S6). Overall, due to mainly the aqueous-phase production of secondary coating components, comparing to campaign-average values, the average *R*<sub>BC</sub> during FE became larger (5.5 vs. 5.0), the OA became more oxygenated (O/C of 0.18 vs. 0.15), and size distributions of OA, sulfate and nitrate all shifted to larger peak sizes (Fig. S5aS7a).

On the other hand, for SE, even though it also occurred during nighttime, the average RH was significantly low (~47%), and it was overwhelmingly dominated by primary species (50.6% of FFOA, 15.2% of BBOA and 18% of BC). Secondary sulfate and nitrate only occupied 2.5% and 2.2% of the total mass of BC-containing particles. Nighttime aqueous-phase related OOA1 contribution was nearly negligible (only 0.8%), which in another way, manifests that during nighttime-efficient OOA1 production was strongly associated with high RH conditions. Due to the contribution of fresh primary emissions, the coating OA was less oxygenated than that of campaign-averaged OA (O/C of 0.12 vs. 0.15), and the average *R*<sub>BC</sub> during SE was consistently smaller (4.5 vs. 5.0). Mass spectrum of BC-Org (Fig. 7b) also contained significant PAHs fragments, in line with the large contribution from FFOA (mainly coal combustion). Average size distribution of OA during SE was broader and peaked in a smaller diameter (<500 nm *D*<sub>va</sub>) (Fig. S5bS7b), in response to the dominance of POA. Occurrence of the highly polluted SE demonstrates that even though the pollutions of BC-containing particles in urban Beijing during winter are on average governed by secondary species, local primary emissions sometimes can lead to serious and short-term pollution events as well.

#### 4. Conclusions

As part of the UK-China 2016 APHH winter campaign, for the first time, an Aerodyne SP-AMS was introduced to exclusively determine the chemical compositions of BC-containing particles in urban Beijing. We found the average concentrations of BC and its coating species were 4.9 and 24.5 μg m<sup>-3</sup>, namely therefore the *R*<sub>BC</sub> (mass ratio of coating to BC) was ~5.0. The coating was dominated by organics (59.4% of total mass of BC-containing particles), followed by nitrate and sulfate (15.3%

带格式的: 字体: 非倾斜

带格式的: 字体: 非倾斜

together). Size distribution data ~~demonstrated~~demonstrates that larger BC-containing particles tend to have thicker coating, more secondary species and more internally mixed coating components. PMF analyses of organic coating further identified two POA factors ~~related~~relevant with fossil fuel and biomass burning, respectively, which dominated the total OA mass. Two SOA factors were also separated, and both of them were found to be mainly contributed by photochemical activities, besides a fraction of the highly oxidized OA factor could be produced by nighttime aqueous-phase reactions. In addition, significant photochemical formation of nitrate rather than sulfate in the afternoon was observed.

Comparisons of the coating compositions between clean and pollution periods shows the critically important role of chemical aging for the pollution of BC-containing particles in urban Beijing. We also found that in one case, aqueous-phase production might lead to serious pollution under high RH conditions, while in another case, fossil fuel combustion could cause extreme and short-term heavy pollution. Comparisons between the BC-containing particles and the total submicron aerosol particles during this campaign will be presented in details in near future.

## Acknowledgements

This work was supported by the National Key R&D program of China (2016YFC0203501), the Natural Science Foundation of China (21777073, 91544220, 21577065, and 41571130034,), ~~and~~ the International ST Cooperation Program of China (2014DFA90780), and the UK Natural Environment Research Council (grant ref. NE/N00695X/1).

## References

- Aiken, A. C., Decarlo, P. F., Kroll, J. H., Worsnop, D. R., Huffman, J. A., Docherty, K. S., Ulbrich, I. M., Mohr, C., Kimmel, J. R., Sueper, D., Sun, Y., Zhang, Q., Trimborn, A., Northway, M., Ziemann, P. J., Canagaratna, M. R., Onasch, T. B., Alfarra, M. R., Prevot, A. S. H., Dommen, J., Duplissy, J., Metzger, A., Baltensperger, U., and Jimenez, J. L.: O/C and OM/OC ratios of primary, secondary, and ambient organic aerosols with high-resolution time-of-flight aerosol mass spectrometry, *Environ. Sci. Tech.*, 42, 4478-4485, 2008.
- Bond, T. C., Doherty, S. J., Fahey, D. W., Forster, P. M., Berntsen, T., DeAngelo, B. J., Flanner, M. G., Ghan, S., Kärcher, B., Koch, D., Kinne, S., Kondo, Y., Quinn, P. K., Sarofim, M. C., Schultz, M. G., Schulz, M., Venkataraman, C., Zhang, H., Zhang, S., Bellouin, N., Guttikunda, S. K., Hopke, P. K., Jacobson, M. Z., Kaiser, J. W., Klimont, Z., Lohmann, U., Schwarz, J. P., Shindell, D., Storelvmo, T., Warren, S. G., and Zender, C. S.: Bounding the role of black carbon in the climate system: A scientific assessment, *J. Geophys. Res.-Atmos.*, 118, 5380-5552, 2013.
- Canagaratna, M. R., Jayne, J. T., Jimenez, J. L., Allan, J. D., Alfarra, M. R., Zhang, Q., Onasch, T. B., Drewnick, F., Coe, H., Middlebrook, A., Delia, A., Williams, L. R., Trimborn, A. M., Northway, M. J., Decarlo, P. F., Kolb, C. E.,

Davidovits, P., and Worsnop, D. R.: Chemical and microphysical characterization of ambient aerosols with the aerodyne aerosol mass spectrometer, *Mass Spectrom. Rev.*, 26, 185-222, 2007.

Canagaratna, M. R., Massoli, P., Browne, E. C., Franklin, J. P., Wilson, K. R., Onasch, T. B., Kirchstetter, T. W., Fortner, E. C., Kolb, C. E., Jayne, J. T., Kroll, J. H., and Worsnop, D. R.: Chemical compositions of black carbon particle cores and coatings via soot particle aerosol mass spectrometry with photoionization and electron ionization, *J. Phys. Chem. A*, 119, 4589-4599, 2015.

Cappa, C. D., Onasch, T. B., Massoli, P., Worsnop, D. R., Bates, T. S., Cross, E. S., Davidovits, P., Hakala, J., Hayden, K. L., Jobson, B. T., Kolesar, K. R., Lack, D. A., Lerner, B. M., Li, S.-M., Mellon, D., Nuaaman, I., Olfert, J. S., Petäjä, T., Quinn, P. K., Song, C., Subramanian, R., Williams, E. J., and Zaveri, R. A.: Radiative absorption enhancements due to the mixing state of atmospheric black carbon, *Science*, 337, 1078-1081, 2012.

Chen, C., Fan, X., Shaltout, T., Qiu, C., Ma, Y., Goldman, A., and Khalizov, A. F.: An unexpected restructuring of combustion soot aggregates by subnanometer coatings of polycyclic aromatic hydrocarbons, *Geophys. Res. Lett.*, 43, 11080-11088, 2016a.

Chen, Y., Schleicher, N., Fricker, M., Cen, K., Liu, X.-l., Kaminski, U., Yu, Y., Wu, X., and Norra, S.: Long-term variation of black carbon and PM<sub>2.5</sub> in Beijing, China with respect to meteorological conditions and governmental measures, *Environ. Pollut.*, 212, 269-278, 2016b.

Cheng, Y., He, K.-b., Engling, G., Weber, R., Liu, J., Du, Z.-y., and Dong, S.-p.: Brown and black carbon in Beijing aerosol: Implications for the effects of brown coating on light absorption by black carbon, *Sci. Total. Environ.*, 599-600, 1047-1055, 2017.

Collier, S., Williams, L. R., Onasch, T. B., Cappa, C. D., Zhang, X., Russell, L. M., Chen, C.-L., Sanchez, K. J., Worsnop, D. R., and Zhang, Q.: Influence of emissions and aqueous processing on particles containing black carbon in a polluted urban environment: insights from a soot particle-aerosol mass spectrometer, *J. Geophys. Res.-Atmos.*, 123, 6648-6666, 2018.

Cubison, M. J., Ortega, A. M., Hayes, P. L., Farmer, D. K., Day, D., Lechner, M. J., Brune, W. H., Apel, E., Diskin, G. S., Fisher, J. A., Fuelberg, H. E., Hecobian, A., Knapp, D. J., Mikoviny, T., Riemer, D., Sachse, G. W., Sessions, W., Weber, R. J., Weinheimer, A. J., Wisthaler, A., and Jimenez, J. L.: Effects of aging on organic aerosol from open biomass burning smoke in aircraft and laboratory studies, *Atmos. Chem. Phys.*, 11, 12049-12064, 2011.

Cui, X., Wang, X., Yang, L., Chen, B., Chen, J., Andersson, A., and Gustafsson, Ö.: Radiative absorption enhancement from coatings on black carbon aerosols, *Sci. Total Environ.*, 551-552, 51-56, 2016.

Ding, A. J., Huang, X., Nie, W., Sun, J. N., Kerminen, V. M., Petäjä, T., Su, H., Cheng, Y. F., Yang, X. Q., Wang, M. H., Chi, X. G., Wang, J. P., Virkkula, A., Guo, W. D., Yuan, J., Wang, S. Y., Zhang, R. J., Wu, Y. F., Song, Y., Zhu, T., Zilitinkevich, S., Kulmala, M., and Fu, C. B.: Enhanced haze pollution by black carbon in megacities in China, *Geophys. Res. Lett.*, 43, 2873-2879, 2016.

Dusek, U., Reischl, G. P., and Hitztenberger, R.: CCN activation of pure and coated carbon black particles, *Environ. Sci. Tech.*, 40, 1223-1230, 2006.

Dusek, U., Frank, G. P., Curtius, J., Drewnick, F., Schneider, J., Kurten, A., Rose, D., Andreae, M. O., Borrmann, S., and Pöschl, U.: Enhanced organic mass fraction and decreased hygroscopicity of cloud condensation nuclei (CCN) during new particle formation events, *Geophys. Res. Lett.*, 37 (3) :174-180, 2010.

Ervens, B., Turpin, B. J., and Weber, R. J.: Secondary organic aerosol formation in cloud droplets and aqueous particles (aqSOA): a review of laboratory, field and model studies, *Atmos. Chem. Phys.*, 11, 22301-22383, 2011.

Ge, X., Zhang, Q., Sun, Y., Ruehl, C. R., and Setyan, A.: Effect of aqueous-phase processing on aerosol chemistry and size distributions in Fresno, California, during wintertime, *Environ. Chem.*, 9, 221-235, 2012.

Ge, X., He, Y., Sun, Y., Xu, J., Wang, J., Shen, Y., and Chen, M.: Characteristics and formation mechanisms of fine particulate nitrate in typical urban areas in china, *Atmosphere*, 8, 62, 2017a.

461 Ge, X., Li, L., Chen, Y., Chen, H., Wu, D., Wang, J., Xie, X., Ge, S., Ye, Z., Xu, J., and Chen, M.: Aerosol characteristics  
 462 and sources in Yangzhou, China resolved by offline aerosol mass spectrometry and other techniques, *Environ. Pollut.*,  
 463 225, 74-85, 2017b.

464 Hermann, H., Schaefer, T., Tilgner, A., Styler, S. A., Weller, C., Teich, M., and Otto, T.: Tropospheric aqueous-phase  
 465 chemistry: kinetics, mechanisms, and its coupling to a changing gas phase, *Chem. Rev.*, 115, 4259, 2015.

466 Huang, R.-J., Zhang, Y., Bozzetti, C., Ho, K.-F., Cao, J.-J., Han, Y., Daellenbach, K. R., Slowik, J. G., Platt, S. M., Canonaco,  
 467 F., Zotter, P., Wolf, R., Pieber, S. M., Bruns, E. A., Crippa, M., Ciarelli, G., Piazzalunga, A., Schwikowski, M.,  
 468 Abbaszade, G., Schnelle-Kreis, J., Zimmermann, R., An, Z., Szidat, S., Baltensperger, U., Haddad, I. E., and Prévôt,  
 469 A. S. H.: High secondary aerosol contribution to particulate pollution during haze events in China, *Nature*, 514, 218-  
 470 222, 2014.

471 Jacobson, M. Z.: Strong radiative heating due to the mixing state of black carbon in atmospheric aerosols. *Nature*, 409,  
 472 695-697, 2001.

473 Jayne, J. T., Leard, D. C., Zhang, X., Davidovits, P., Smith, K. A., Kolb, C. E., and Worsnop, D. R.: Development of an  
 474 aerosol mass spectrometer for size and composition analysis of submicron particles, *Aerosol Sci. Tech.*, 33, 49 - 70,  
 475 2000.

476 Ji, D., Li, L., Pang, B., Xue, P., Wang, L., Wu, Y., Zhang, H., and Wang, Y.: Characterization of black carbon in an urban-  
 477 rural fringe area of Beijing, *Environ. Pollut.*, 223, 524-534, 2017.

478 Kroll, J.H., Donahue, N.M., Jimenez, J.L., Kessler, S.H., Canagaratna, M.R., Wilson, K.R., Altieri, K.E., Mazzoleni, L.R.,  
 479 Wozniak, A.S., Bluhm, H., Mysak, E.R., Smith, J.D., Kolb, C.E., Worsnop, D.R.: Carbon oxidation state as a metric  
 480 for describing the chemistry of atmospheric organic aerosol. *Nat. Chem.* 3, 133-139, 2011.

481 [Kuang, Y., Zhao, C. S., Ma, N., Liu, H. J., Bian, Y. X., Tao, J. C., and Hu, M.: Deliquescent phenomena of ambient aerosols  
 482 on the North China Plain, \*Geophys. Res. Lett.\*, 43, 8744-8750, 2016.](#)

483 Laborde, M., Schnaiter, M., Linke, C., Saathoff, H., Naumann, K., Möhler, O., Berlenz, S., Wagner, U., Taylor, J., and Liu,  
 484 D.: Single particle soot photometer intercomparison at the AIDA chamber, *Atmos. Meas. Tech.*, 5, 3077-3097, 2012.

485 Lee, A. K. Y., Willis, M. D., Healy, R. M., Onasch, T. B., and Abbatt, J. P. D.: Mixing state of carbonaceous aerosol in an  
 486 urban environment: single particle characterization using the soot particle aerosol mass spectrometer (SP-AMS),  
 487 *Atmos. Chem. Phys.*, 15, 1823-1841, 2015.

488 Lee, A. K. Y., Chen, C. L., Liu, J., Price, D. J., Betha, R., Russell, L. M., Zhang, X., and Cappa, C. D.: Formation of  
 489 secondary organic aerosol coating on black carbon particles near vehicular emissions, *Atmos. Chem. Phys.*, 2017, 1-  
 490 20, 2017.

491 [Li, W., Sun, J., Xu, L., Shi, Z., Riemer, N., Sun, Y., Fu, P., Zhang, J., Lin, Y., Wang, X., Shao, L., Chen, J., Zhang, X., Wang,  
 492 Z., and Wang, W.: A conceptual framework for mixing structures in individual aerosol particles, \*J. Geophys. Res. -  
 493 Atmos.\*, 121, 13784-13798, 2016.](#)

494 Liu, D., Allan, J., Whitehead, J., Young, D., Flynn, M., Coe, H., McFiggans, G., Fleming, Z. L., and Bandy, B.: Ambient  
 495 black carbon particle hygroscopic properties controlled by mixing state and composition, *Atmos. Chem. Phys.*, 13,  
 496 2015-2029, 2013.

497 Liu, D., Whitehead, J., Alfarra, M. R., Reyes-Villegas, E., Spracklen, D. V., Reddington, C. L., Kong, S., Williams, P. I.,  
 498 Ting, Y.-C., Haslett, S., Taylor, J. W., Flynn, M. J., Morgan, W. T., McFiggans, G., Coe, H., and Allan, J. D.: Black-  
 499 carbon absorption enhancement in the atmosphere determined by particle mixing state, *Nat. Geosci.*, 10, 184-188,  
 500 2017.

501 [Liu, D., Joshi, R., Wang, J., Yu, C., Allan, J. D., Coe, H., Flynn, M. J., Xie, C., Lee, J., Squires, F., Kotthaus, S., Grimmond,  
 502 S., Ge, X., Sun, Y., and Fu, P.: Contrasting physical properties of black carbon in urban Beijing between winter and  
 503 summer, \*Atmos. Chem. Phys. Discuss.\*, 2018, 1-30, 10.5194/acp-2018-1142, 2018.](#)

504 [Liu, Q., Ma, T., Olson, M. R., Liu, Y., Zhang, T., Wu, Y., and Schauer, J. J.: Temporal variations of black carbon during](#)

haze and non-haze days in Beijing, *Sci. Rep.*, 6, 33331, 2016.

Liu, S., Aiken, A. C., Gorkowski, K., Dubey, M. K., Cappa, C. D., Williams, L. R., Herndon, S. C., Massoli, P., Fortner, E. C., Chhabra, P. S., Brooks, W. A., Onasch, T. B., Jayne, J. T., Worsnop, D. R., China, S., Sharma, N., Mazzoleni, C., Xu, L., Ng, N. L., Liu, D., Allan, J. D., Lee, J. D., Fleming, Z. L., Mohr, C., Zotter, P., Szidat, S., and Prevot, A. S. H.: Enhanced light absorption by mixed source black and brown carbon particles in UK winter, *Nat. Commun.*, 6, 8435, 2015.

Massoli, P., Onasch, T. B., Cappa, C. D., Nuumaan, I., Hakala, J., Hayden, K., Li, S.-M., Sueper, D. T., Bates, T. S., Quinn, P. K., Jayne, J. T., and Worsnop, D. R.: Characterization of black carbon-containing particles from soot particle aerosol mass spectrometer measurements on the R/V Atlantis during CalNex 2010, *J. Geophys. Res.-Atmos.*, 120, 2014JD022834, 2015.

Meng, J., Liu, J., Guo, S., Li, J., Li, Z., and Tao, S.: Trend and driving forces of Beijing's black carbon emissions from sectoral perspectives, *J. Clean. Prod.*, 112, 1272-1281, 2016.

Mohr, C., Huffman, J. A., Cubison, M. J., Aiken, A. C., Docherty, K. S., Kimmel, J. R., Ulbrich, I. M., Hannigan, M., and Jimenez, J. L.: Characterization of primary organic aerosol emissions from meat cooking, trash burning, and motor vehicles with high-resolution aerosol mass spectrometry and comparison with ambient and chamber observations, *Environ. Sci. Tech.*, 43, 2443-2449, 2009.

Onasch, T. B., Trimborn, A., Fortner, E. C., Jayne, J. T., Kok, G. L., Williams, L. R., Davidovits, P., and Worsnop, D. R.: Soot particle aerosol mass spectrometer: development, validation, and initial application, *Aerosol Sci. Tech.*, 46, 804-817, 2012.

Paatero, P., and Tapper, U.: Positive matrix factorization: A non-negative factor model with optimal utilization of error estimates of data values, *Environmetrics*, 5, 111-126, 1994.

Peng, J., Hu, M., Guo, S., Du, Z., Zheng, J., Shang, D., Levy, Z. M., Zeng, L., Shao, M., and Wu, Y. S.: Markedly enhanced absorption and direct radiative forcing of black carbon under polluted urban environments, *P Natl. Acad. Sci. USA*, 113, 4266, 2016.

Pokhrel, R. P., Beamesderfer, E. R., Wagner, N. L., Langridge, J. M., Lack, D. A., Jayarathne, T., Stone, E. A., Stockwell, C. E., Yokelson, R. J., and Murphy, S. M.: Relative importance of black carbon, brown carbon, and absorption enhancement from clear coatings in biomass burning emissions, *Atmos. Chem. Phys.*, 17, 5063-5078, 2017.

Ramanathan, V., and Carmichael, G.: Global and regional climate changes due to black carbon, *Nat. Geosci.*, 1, 221-227, 2008.

Schleicher, N., Cen, K., and Norra, S.: Daily variations of black carbon and element concentrations of atmospheric particles in the Beijing megacity – Part 1: general temporal course and source identification, *Chem Erde Geochem.*, 73, 51-60, 2013a.

Schleicher, N., Norra, S., Fricker, M., Kaminski, U., Chen, Y., Chai, F., Wang, S., Yu, Y., and Cen, K.: Spatio-temporal variations of black carbon concentrations in the Megacity Beijing, *Environ. Pollut.*, 182, 392-401, 2013b.

Shi, Z., Vu, T., Kotthaus, S., Grimmond, S., Harrison, R. M., Yue, S., Zhu, T., Lee, J., Han, Y., Demuzere, M., Dunmore, R. E., Ren, L., Liu, D., Wang, Y., Wild, O., Allan, J., Barlow, J., Beddows, D., Bloss, W. J., Carruthers, D., Carslaw, D. C., Chatzidiakou, L., Crilley, L., Coe, H., Dai, T., Doherty, R., Duan, F., Fu, P., Ge, B., Ge, M., Guan, D., Hamilton, J. F., He, K., Heal, M., Heard, D., Hewitt, C. N., Hu, M., Ji, D., Jiang, X., Jones, R., Kalberer, M., Kelly, F. J., Kramer, L., Langford, B., Lin, C., Lewis, A. C., Li, J., Li, W., Liu, H., Loh, M., Lu, K., Mann, G., McFiggans, G., Miller, M., Mills, G., Monk, P., Nemitz, E., O'Connor, F., Ouyang, B., Palmer, P. I., Percival, C., Popoola, O., Reeves, C., Rickard, A. R., Shao, L., Shi, G., Spracklen, D., Stevenson, D., Sun, Y., Sun, Z., Tao, S., Tong, S., Wang, Q., Wang, W., Wang, X., Wang, Z., Whalley, L., Wu, X., Wu, Z., Xie, P., Yang, F., Zhang, Q., Zhang, Y., Zhang, Y., and Zheng, M.: Introduction to Special Issue – In-depth study of air pollution sources and processes within Beijing and its surrounding region (APHH-Beijing), *Atmos. Chem. Phys. Discuss.*, 2018, 1-62, 10.5194/acp-2018-922, 2018.

549 Song, S., Wu, Y., Xu, J., Ohara, T., Hasegawa, S., Li, J., Yang, L., and Hao, J.: Black carbon at a roadside site in Beijing:  
 550 Temporal variations and relationships with carbon monoxide and particle number size distribution, *Atmos. Environ.*,  
 551 77, 213-221, 2013.

552 Sun, J., Liu, L., Xu, L., Wang, Y., Wu, Z., Hu, M., Shi, Z., Li, Y., Zhang, X., Chen, J., and Li, W.: Key Role of Nitrate in  
 553 Phase Transitions of Urban Particles: Implications of Important Reactive Surfaces for Secondary Aerosol Formation,  
 554 *J. Geophys. Res.-Atmos.*, 123, 1234-1243, 2018.

555 Sun, Y., Jiang, Q., Wang, Z., Fu, P., Li, J., Yang, T., and Yin, Y.: Investigation of the sources and evolution processes of  
 556 severe haze pollution in Beijing in January 2013, *J Geophys. Res.-Atmos.*, 119, 4380-4398, 2014.

557 Sun, Y., Du, W., Fu, P., Wang, Q., Li, J., Ge, X., Zhang, Q., Zhu, C., Ren, L., Xu, W., Zhao, J., Han, T., Worsnop, D. R.,  
 558 and Wang, Z.: Primary and secondary aerosols in Beijing in winter: sources, variations and processes, *Atmos. Chem.*  
 559 *Phys.*, 16, 8309-8329, 2016.

560 Sun, Y., Zhang, Q., Schwab, J. J., Yang, T., Ng, N. L., and Demerjian, K. L.: Factor analysis of combined organic and  
 561 inorganic aerosol mass spectra from high resolution aerosol mass spectrometer measurements, *Atmos. Chem. Phys.*,  
 562 12, 8537-8551, 2012.

563 Ulbrich, I. M., Canagaratna, M. R., Zhang, Q., Worsnop, D. R., and Jimenez, J. L.: Interpretation of organic components  
 564 from Positive Matrix Factorization of aerosol mass spectrometric data, *Atmos. Chem. Phys.*, 9, 2891-2918, 2009.

565 Wang, J., Onasch, T. B., Ge, X., Collier, S., Zhang, Q., Sun, Y., Yu, H., Chen, M., Prévôt, A. S. H., and Worsnop, D. R.:  
 566 Observation of fullerene soot in eastern China, *Environ. Sci. Tech. Lett.*, 3, 121-126, 2016a.

567 Wang, J., Zhang, Q., Chen, M.-D., Collier, S., Zhou, S., Ge, X., Xu, J., Shi, J., Xie, C., Hu, J., Ge, S., Sun, Y., and Coe, H.:  
 568 First chemical characterization of refractory black carbon aerosols and associated coatings over the Tibetan Plateau  
 569 (4730 m a.s.l), *Environ. Sci. Tech.*, 51 (24) :14072, 2017a.

570 Wang, J., Wu, Y., Ge, X., Shen, Y., Ge, S., Chen, M.: Characteristics and sources of ambient refractory black carbon aerosols:  
 571 Insights from soot particle aerosol mass spectrometer. *Atmos. Environ.*, 185, 147-152, 2018.

572 Wang, Q., Huang, R.-J., Cao, J., Tie, X., Shen, Z., Zhao, S., Han, Y., Li, G., Li, Z., Ni, H., Zhou, Y., Wang, M., Chen, Y.,  
 573 and Su, X.: Contribution of regional transport to the black carbon aerosol during winter haze period in Beijing, *Atmos.*  
 574 *Environ.*, 132, 11-18, 2016b.

575 Wang, Y., de Foy, B., Schauer, J. J., Olson, M. R., Zhang, Y., Li, Z., and Zhang, Y.: Impacts of regional transport on black  
 576 carbon in Huairou, Beijing, China, *Environ. Pollut.*, 221, 75-84, 2017b.

577 Wang, Y., Liu, F., He, C., Bi, L., Cheng, T., Wang, Z., Zhang, H., Zhang, X., Shi, Z., and Li, W.: Fractal dimensions and  
 578 mixing structures of soot particles during atmospheric processing, *Environ. Sci. Technol. Lett.*, 4, 487-493, 2017c.

579 Willis, M. D., Lee, A. K. Y., Onasch, T. B., Fortner, E. C., Williams, L. R., Lambe, A. T., Worsnop, D. R., and Abbatt, J. P.  
 580 D.: Collection efficiency of the Soot-Particle Aerosol Mass Spectrometer (SP-AMS) for internally mixed particulate  
 581 black carbon, *Atmos. Meas. Tech.*, 7, 5223-5249, 2014.

582 Willis, M. D., Healy, R. M., Riemer, N., West, M., Wang, J. M., Jeong, C. H., Wenger, J. C., Evans, G. J., Abbatt, J. P. D.,  
 583 and Lee, A. K. Y.: Quantification of black carbon mixing state from traffic: implications for aerosol optical properties,  
 584 *Atmos. Chem. Phys.*, 16, 4693-4706, 2016.

585 Wu, Y., Zhang, R., Tian, P., Tao, J., Hsu, S. C., Yan, P., Wang, Q., Cao, J., Zhang, X., and Xia, X.: Effect of ambient  
 586 humidity on the light absorption amplification of black carbon in Beijing during January 2013, *Atmos Environ.*, 124,  
 587 217-223, 2016.

588 Wu, Y., Wang, X., Tao, J., Huang, R., Tian, P., Cao, J., Zhang, L., Ho, K. F., Han, Z., and Zhang, R.: Size distribution and  
 589 source of black carbon aerosol in urban Beijing during winter haze episodes, *Atmos. Chem. Phys.*, 17, 7965-7975,  
 590 2017.

591 Wu, Z., Wang, Y., Tan, T., Zhu, Y., Li, M., Shang, D., Wang, H., Lu, K., Guo, S., Zeng, L., and Zhang, Y.: Aerosol liquid  
 592 water driven by anthropogenic inorganic salts: Implying its key role in haze formation over the North China Plain.

Environ. Sci. Technol. Lett., 5, 160-166, 2018.

Xie, C., Xu, W., Wang, J., Wang, Q., Liu, D., Tang, G., Chen, P., Du, W., Zhao, J., Zhang, Y., Zhou, W., Han, T., Bian, Q., Li, J., Fu, P., Wang, Z., Ge, X., Allan, J., Coe, H., and Sun, Y.: Vertical characterization of aerosol optical properties and brown carbon in winter in urban Beijing, China, Atmos. Chem. Phys. Discuss., 2018, 1-28, 10.5194/acp-2018-788, 2018.

Xu, W., Han, T., Du, W., Wang, Q., Chen, C., Zhao, J., Zhang, Y., Li, J., Fu, P., Wang, Z., Worsnop, D. R., and Sun, Y.: Effects of aqueous-phase and photochemical processing on secondary organic aerosol formation and evolution in Beijing, China, Environ. Sci. Tech., 51, 762-770, 2017.

Yan, C., Zheng, M., Sullivan, A. P., Shen, G., Chen, Y., Wang, S., Zhao, B., Cai, S., Desyaterik, Y., Li, X., Zhou, T., Gustafsson, Ö., and Collett, J. L.: Residential coal combustion as a source of levoglucosan in China, Environ. Sci. Tech., 52, 1665-1674, 2018.

Yang, T., Guilin, H., and Zhifang, X.: Atmospheric Black Carbon Deposit in Beijing and Zhangbei, China, Procedia Earth and Planet. Sci., 10, 383-387, 2014.

Zhang, Q., Alfarra, M. R., Worsnop, D. R., Allan, J. D., Coe, H., Canagaratna, M. R., and Jimenez, J. L.: Deconvolution and quantification of hydrocarbon-like and oxygenated organic aerosols based on aerosol mass spectrometry, Environ. Sci. Tech., 39, 4938-4952, 2005.

Zhang, Q., Jimenez, J., Canagaratna, M., Ulbrich, I., Ng, N., Worsnop, D., and Sun, Y.: Understanding atmospheric organic aerosols via factor analysis of aerosol mass spectrometry: a review, Anal. Bioanal. Chem., 401, 3045-3067, 2011.

Zhang, S., Wu, Y., Yan, H., Du, X., Max Zhang, K., Zheng, X., Fu, L., and Hao, J.: Black carbon pollution for a major road in Beijing: Implications for policy interventions of the heavy-duty truck fleet, Transport. Res. D-TR E, 2017.



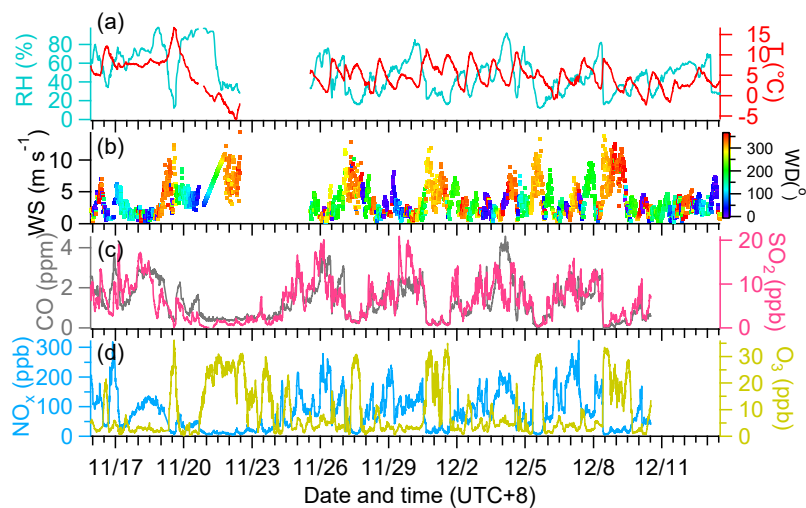
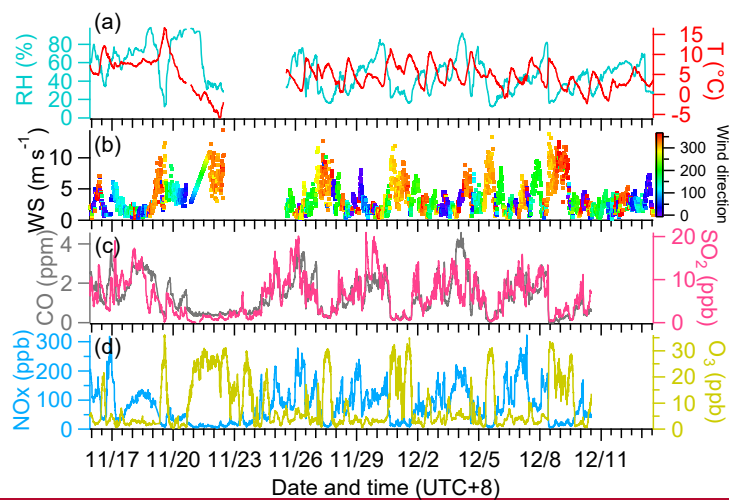
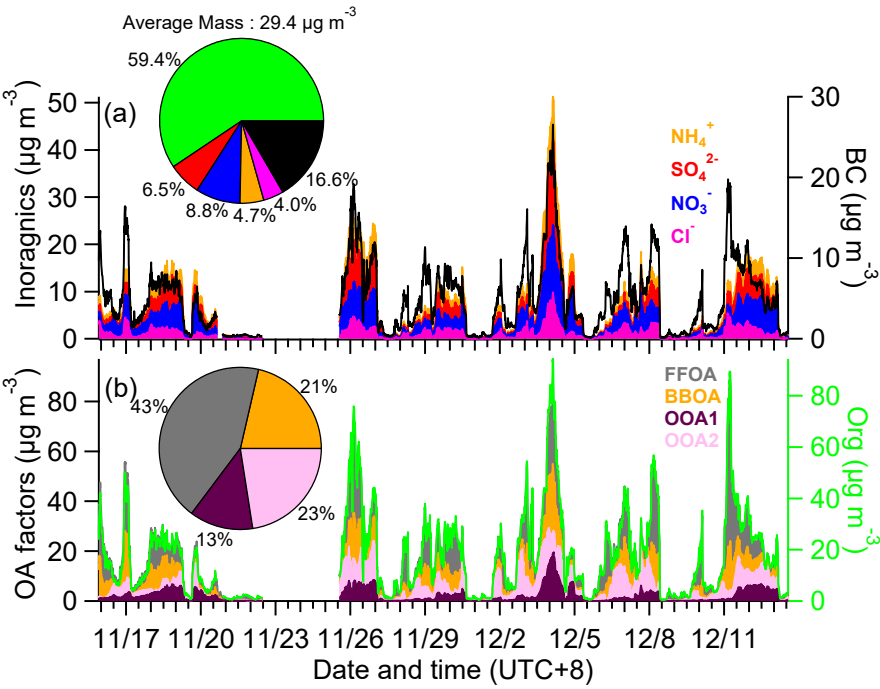


Figure 1. Temporal variation of (a) relative humidity (RH) and temperature (T, °C), (b) wind speed (WS, m s<sup>-1</sup>) and wind direction (WD), and (c)(d) mass loadings of CO, SO<sub>2</sub>, NO<sub>x</sub> and O<sub>3</sub>.



621 Figure 2. (a) Temporal variations of mass loadings of inorganic coating components (sulfate, nitrate, ammonium and  
622 chloride) and BC cores, and (b) temporal variations of mass loadings of organic coating (Org) and PMF separated OA  
623 factors (inset pie charts show the average composition of total BC-containing particles; and organics, respectively).  
624

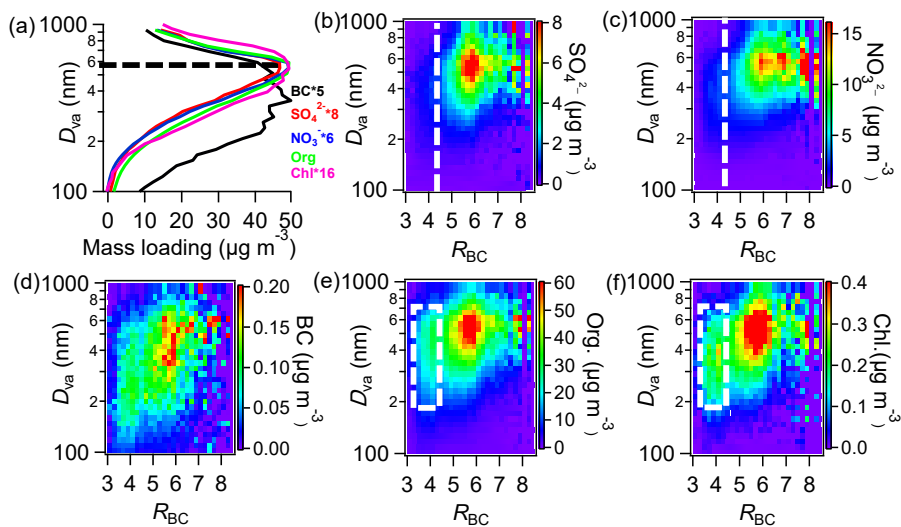
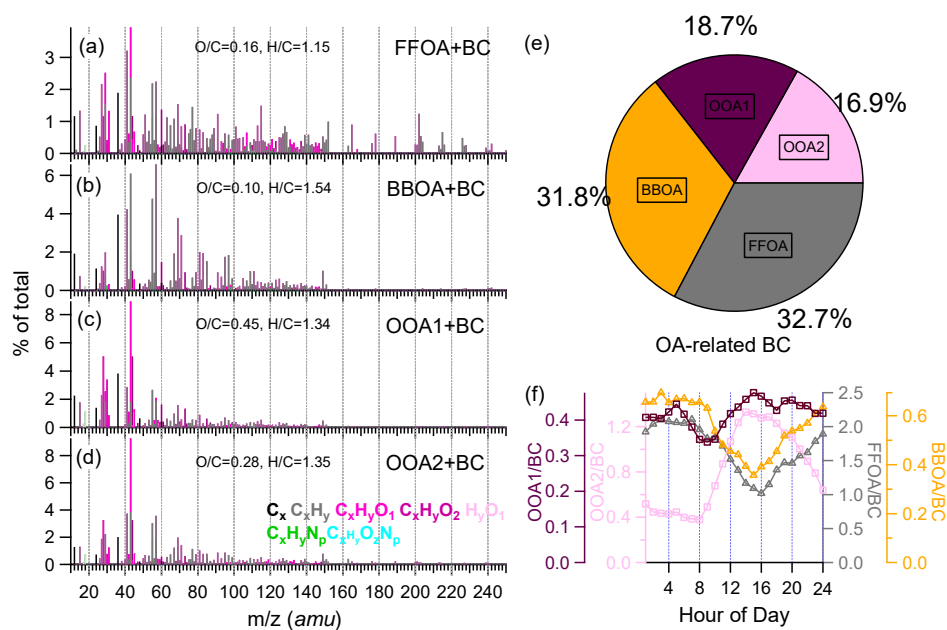
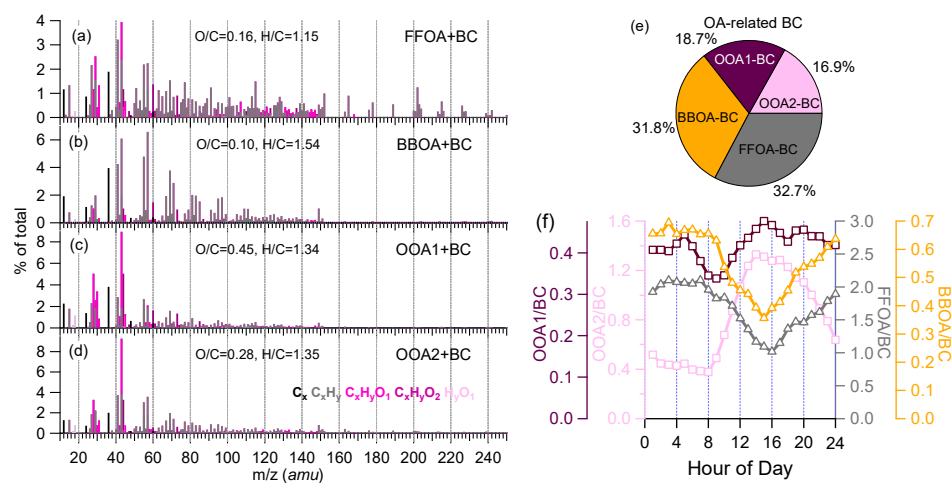


Figure 3. Mass-based campaign-averaged size distributions: (a) major coating components and BC cores, and (b-f) image plots of size distributions of sulfate, nitrate, BC, organics, and chloride as a function of  $R_{BC}$  (mass ratio of coating-to-BC) (Note size distributions of BC and chloride were scaled from those of  $m/z$  24 and  $m/z$  35, respectively)

630

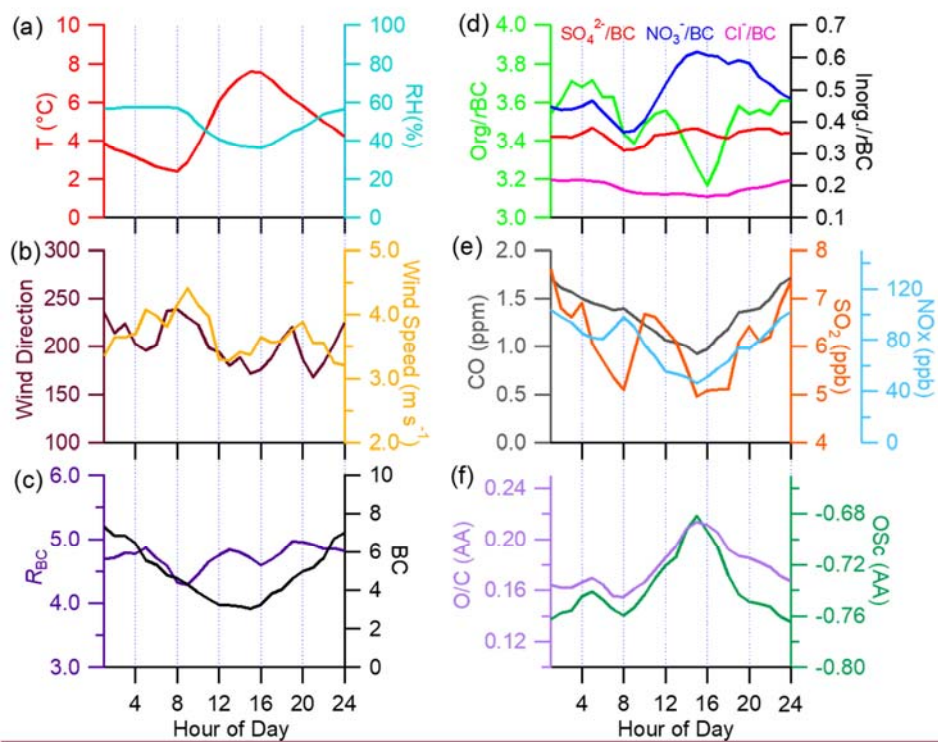


631

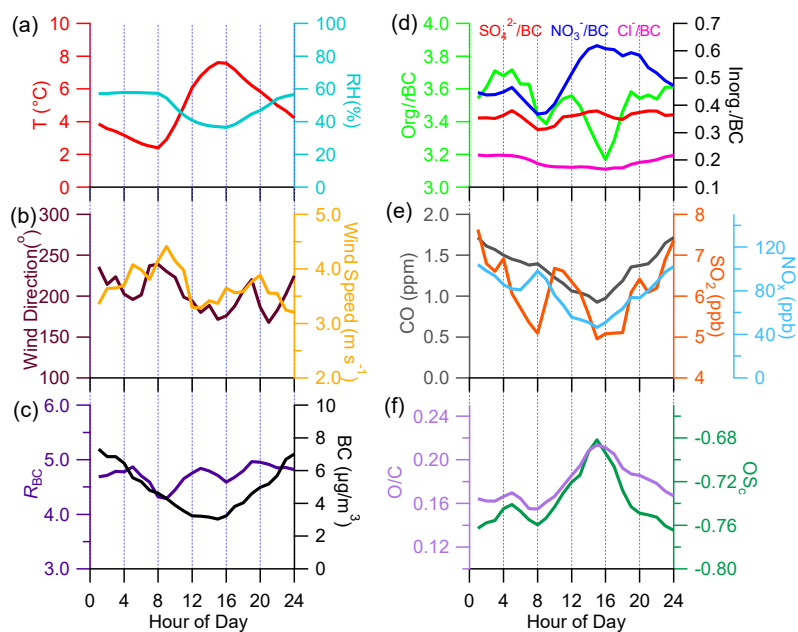


632

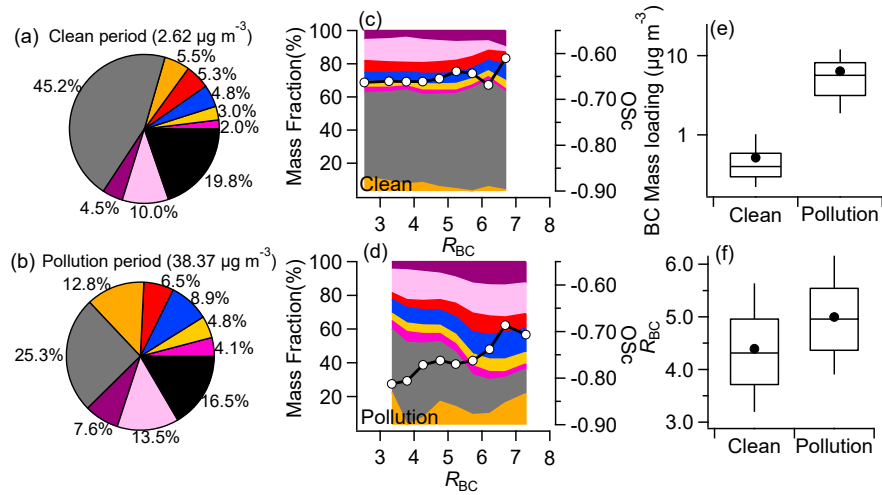
633 Figure 4. High-resolution mass spectra of (a) fossil fuel combustion OA (FFOA + BC), (b) biomass burning OA (BBOA +  
 634 BC), (c) OOA1 + BC, (d) OOA2 + BC, (e) Mass fractions of the BC fragments apportioned in different OA factors, and (f)  
 635 diurnal cycles of the four OA factors relative to BC.  
 636



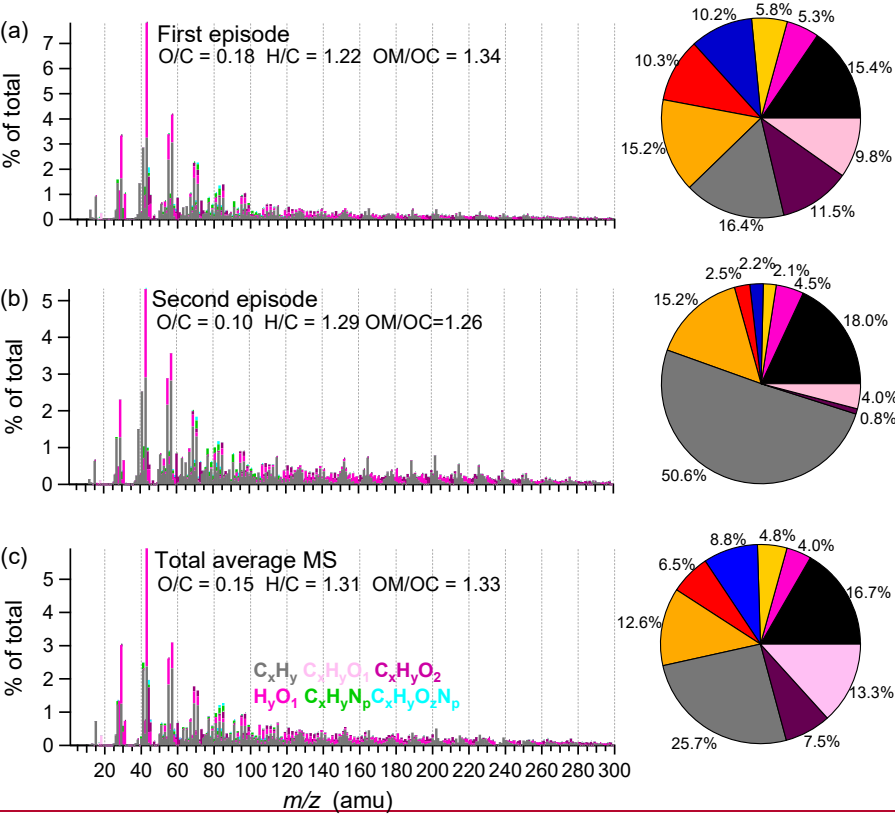
637  
638



641 Figure 5. Diurnal cycles of (a) T and RH, (b) wind direction and wind speed, (c) mass ratio of coatings to BC ( $R_{BC}$ ) and  
 642 BC, (d) Org/BC,  $\text{SO}_4^{2-}/\text{BC}$ ,  $\text{NO}_3^-/\text{BC}$  and  $\text{Cl}^-/\text{BC}$ , (e) mass loadingloadings of gaseous species (CO, SO<sub>2</sub>, NO<sub>x</sub>), and (f) O/C  
 643 and oxidation state ( $OS_c=2*\text{O}/\text{C}-\text{H}/\text{C}$ ).  
 644



647 Figure 6. (a)(b) Average compositions of BC-containing particles during clean and pollution periods, (c)(d) mass fractions  
648 of the non-BC coating components (left y-axis) and  $\text{OS}_c$  (right y-axis) during clean and pollution periods as a function of  
649  $R_{\text{BC}}$ , box plots of BC mass loadings (e) and  $R_{\text{BC}}$  during clean and pollution periods (colors of the components are consistent  
650 with those in Fig. 2).  
651





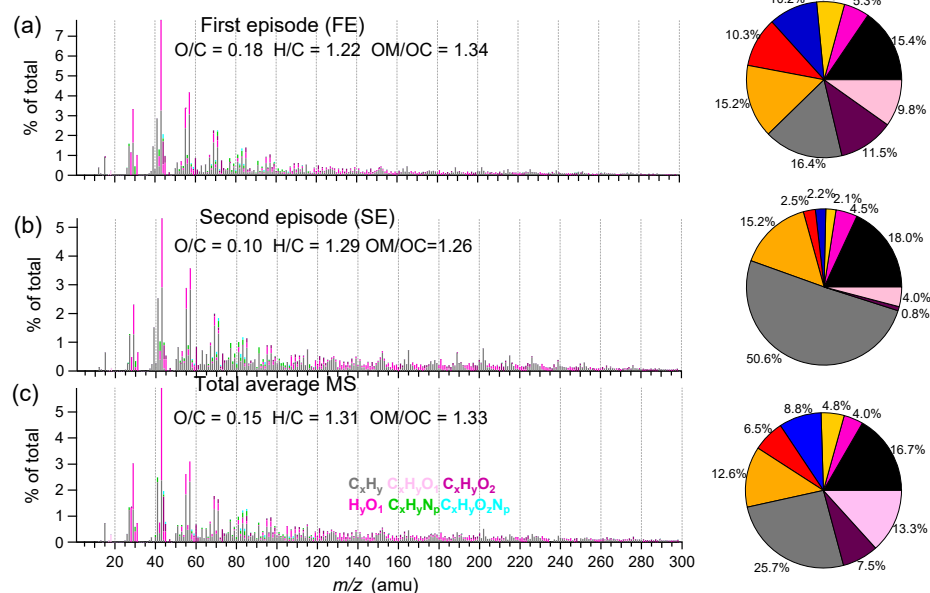


Figure 7. High-resolution mass spectra of the average OA at different episodes: (a) first episode (FE), (b) second episode (SE) and (c) whole campaign (inset pies show the average compositions during corresponding episodes; colors of different components are consistent with those in Fig. 2).